Available online at www.sciencedirect.com
ScienceDirect
Journal of Power Sources 174 (2007) 1121–1125
JOURNAL OF POWER SOURCES
www.elsevier.com/locate/jpowsour

Short communication

Capacity loss in rechargeable lithium cells during cycle life testing: The importance of determining state-of-charge

Matthieu Dubarry, Vojtech Svoboda, Ruey Hwu, Bor Yann Liaw *

Hawaii Natural Energy Institute, School of Ocean and Earth Science and Technology, University of Hawaii at Manoa, 1680 East West Road, POST 109, Honolulu, HI 96822, USA

Available online 30 June 2007

Abstract

Determining state-of-charge (SoC) in a battery has been an important subject for the industry for decades. Despite significant efforts in the past focusing on methodologies to accurately estimate SoC in a battery, the fundamental understanding of the SoC issue has not been clear, at least in the industry where testing, control, and operation are concerned. Recently, we have been working on developing reliable techniques to identify capacity loss mechanism in rechargeable lithium batteries and to quantify contributions to capacity loss from different origins. That prompted us to re-visit the SoC issue. Strictly speaking, SoC is a static thermodynamic property of battery chemistry, which should be determined at equilibrium. On the other hand, cell capacity is a quantity of practical interest often determined by kinetics; thus, it is rate dependent. We conducted a few experiments to illustrate the accurate estimate of SoC through proper measurements. We also explained the proper correlation between SoC and rate capacity. A better understanding of the charge and discharge behavior in a battery under different rates in relation to the SoC is therefore derived.

Keywords: Capacity loss; Rechargeable lithium batteries; Cycle life; State of charge; Rate capacity; Service life prediction

1. Introduction

A very important step in predicting battery service life is to quantify contributions to capacity loss during the life of battery operation. A quantitative identification of various attributes to capacity loss in commercial cells under laboratory evaluation is a significant step toward that goal. An ultimate goal of our approach is to enhance the convenience, reliability, utility, and mobility of a power source in real-life applications. To date, predicting battery service life in practical applications remains problematic due to the lack of well-established and reliable techniques to enable such prediction. Recently, we began to employ protocols used in conventional cycle life tests for cell evaluation; including those using constant current charge and discharge regimes, measurements of equilibrium open circuit voltage (OCV) of the cell, and incremental capacity analysis (ICA) [1]. We were able to separate contributions to capacity loss due to intrinsic and extrinsic origins.

Any useful battery life prediction tool is expected to be able to apply laboratory test results to real-life operations. In any attempt to prevail battery life prediction in real life, the first step toward developing such a tool relies on how well a battery's degradation mechanism is understood and proper analysis of capacity loss mechanism becomes feasible.

With this objective in mind, we thus developed a combination of "close-to-equilibrium" OCV (*cte*-OCV) measurements and ICA to analyze capacity loss in batteries for better mechanistic understanding of the cell chemistry and degradation [1]. This capacity loss analysis allowed us separate undercharging (UC) and underdischarging (UD) issues from degradation of active materials that led to capacity fade. In our approach, the equilibrium OCV measurements can accurately determine the state-of-charge (SoC) of the cell. With high sensitivity, the ICA can detect capacity loss from different contributions, including improper charging or discharging. Similar techniques have been used by others (e.g. [2–4]) to analyze lithium intercalation in cathode materials in the past, but their main interests have been focused more on material characterizations or the related electrode reactions. Not much has been used for cell testing or quantification of capacity or power loss for mechanistic

* Corresponding author. Tel.: +1 808 956 2339; fax: +1 808 956 2336.
E-mail address: bliaw@hawaii.edu (B.Y. Liaw).

0378-7753/$ – see front matter © 2007 Elsevier B.V. All rights reserved.
doi:10.1016/j.jpowsour.2007.06.185

understanding. As we combining these two techniques for cell evaluations, we were able to correlate the capacity loss with an accurately estimated SoC; thus, we can separate certain origins of capacity loss and quantify the amount of contribution from each, including undercharging and underdischarging in battery operation [1].

Since one of the key issues to develop such a predictive tool is to correlate the capacity loss with the SoC, determining SoC in the battery chemistry accurately is a necessity. However, a consistent and reliable method is still missing. The difficulty lies in the fact that the commonly used SoC term is determined by the cell capacity (e.g. [5]), through which it is very difficult to find a reference point to allow reliable SoC inference. Therefore, to date, no matter how intelligent an inference method is used, the uncertainty on SoC remains. We shall call the SoC determined by the capacity-based methods (e.g. coulomb counting with various kinds of curve fitting, from least square estimate to fuzzy-neural inference [6–11]) "engineering-SoC," or "e-SoC". The e-SoC suffers a common problem in its inability to accurately define the "state" of the battery, because it does not correspond to a well-defined relationship with the battery's composition and the extent of reaction in the active materials. True SoC is supposed to be a thermodynamic property of the system [1]; therefore, it should be defined by thermodynamic conditions and constraints; thus, by the composition of the active materials defined by the phase relationship in the system. We shall call SoC determined by the thermodynamic constraints a "thermodynamic-SoC" or "t-SoC." In order to infer the correct SoC, t-SoC needs to be used. A known technique that can determine t-SoC is the equilibrium coulombic titration (ECT) [12–16], which usually involves changing the composition of the active materials in the system potentiostatically or galvanostatically, followed by an equilibrium OCV measurement to determine the potential of the system against a well-established state at the reference electrode. The potentiostatic intermittent titration technique (PITT) and the galvanostatic intermittent titration technique (GITT) [12,13] are two well-established techniques suitable for this purpose. This is the most important aspect in our application of the *cte*-OCV measurement to determine the t-SoC in the cell during cycle life evaluation.

It should be emphasized that most capacity loss involves the changes not only in the thermodynamic aspects but also in the kinetic aspects of a battery. Therefore, to understand loss mechanisms, we need to identify both thermodynamic and kinetic origins that cause the capacity loss. In other words, accurate understanding of the loss mechanism and reliable prediction of its impact on the battery life can only come true with proper correlation of capacity loss with t-SoC.

Extending this knowledge to battery life modeling and prediction, we need to emphasize the importance of using the proper SoC correspondence in the model treatment. For instance, in our recent effort to use an equivalent circuit model to simulate battery performance and life prediction [17–19], we realized the importance of a precise SoC determination in order to utilize correct parameters in the model for an accurate prediction and validation of the battery chemistry [1,19].

In this work, we use experimental results obtained from the evaluation of commercial lithium ion cells to depict the importance of the SoC determination and how to interpret the correct SoC from the experimental data.

2. Experimental

Commercial 2.0 Ah graphite|Li_xCoO_2-based (LCO) 18650 cells manufactured in the same lot were received from a commercial manufacturer. Upon reception, the cells were physically examined, weighted, and stored for further evaluation. Before any evaluation, the cells were conditioned for five cycles with a charge process recommended by the manufacturer and a discharge regime at *C*/5 rate to determine its rate-dependent capacity using a Solartron 1470 station. A cell that has been conditioned and met with product specification was then used to run a few charge and discharge cycles at *C*/3, *C*/5, and *C*/25 rates, as shown in Fig. 1. The capacities at *C*/25, *C*/5 and *C*/3 (denoted as C_{25}, C_5, and C_3, respectively) were measured with the same end-of-charge voltage (EoCV) at 4.2 V and end-of-discharge voltage (EoDV) at 2.8 V. The C_{25} and the associated charge and discharge curves were used to establish the performance baseline and as the basis for the SoC determination. Although a precise OCV versus SoC curve should be determined by PITT or GITT, a sufficiently accurate approximation may be obtained by taking the average potential between the charge and discharge branch at *C*/25 and the normalized C_{25} capacity as a "close-to-equilibrium" SoC to yield a *cte*-OCV versus *cte*-SoC curve and use it as the good-faith OCV versus SoC curve.

3. Results and discussion

Fig. 1 shows the charge and discharge curves and the capacities measured in a LCO cell at *C*/25, *C*/5 and *C*/3 rates. The cell exhibits a strong dependence of polarization, and capacity as well, on the rate. As revealed in the test, more than 30% of the C_{25} capacity is not accessible when the cell was cycled at *C*/3. Fig. 1 is a typical representation of cycling test results, in which the same EoCV leads to the belief that the same return of charge (for the same charge regime) has been achieved, thus the cell has been assumed to return to the same "fully charged

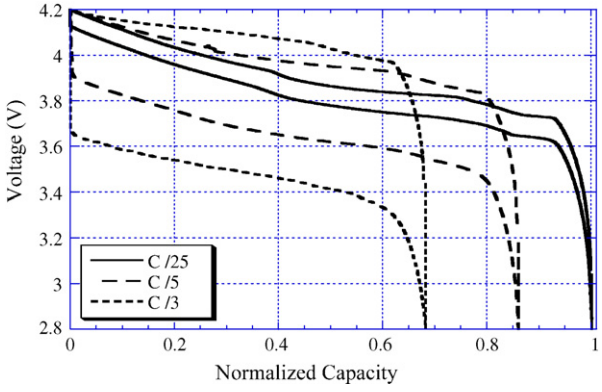

Fig. 1. Charge and discharge curves of a commercial 18650 $LiCoO_2$ (LCO) cell at different rates.

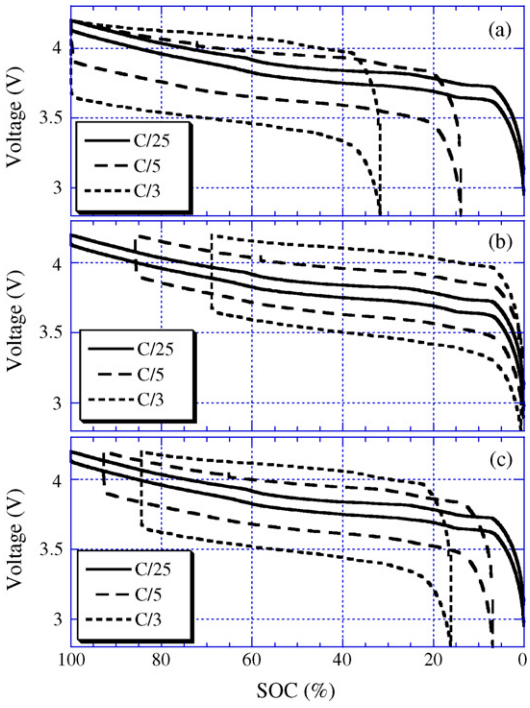

Fig. 2. (a–c) Different interpretations of the relationship between cell voltage (and capacity) and SoC measured in the LCO cell.

state." By convention, this "fully charged state" is considered 100% SoC. The question is whether the "fully charged state" of 100% SoC reached by different charge regimes corresponds to the same t-SoC or not. This intriguing issue remains problematic to date.

To resolve this issue, we shall consider the following three scenarios as posted in Fig. 2 for further discussion.

Scenario (a), as shown in Fig. 2(a), is the same as in Fig. 1 as the conventional representation, in which, even though we do not know if we started each discharge regime from the same "fully charged state," the cell capacity primarily depends on the polarization of the discharge regime. As the polarization overpotential increases with rate, the electrochemical reaction runs to the extent that is determined by kinetics, in accordance with the extent of lithium insertion into the cathode active material (CAM) during discharge. Therefore, the capacity is predominantly determined by the kinetics of the discharge regime (most likely in the cathode, which limits the capacity).

In Scenario (b), as shown in Fig. 2(b), we however rescind the validity of the assumption that the capacity was dominated by the polarization of the cathode reaction. Instead, we consider the sharp voltage drop at the end-of-discharge (EoD) a sign indicating that the cathode reaction was nearly completed, disregarding the discharge rate and the starting composition reached by the charge regime. In other words, we postulate that the characteristic, abrupt voltage drop at the EoD always reflects that the reaction has reached the "completely discharged state." Accordingly, as we line up the charge and discharge curves to the same EoD state, the figure also reveals that the polarization overpotential in the charge and discharge regime is comparable and about the same magnitude. This exhibition intriguingly portrays that the polarization in the charge regime may have determined the end-of-charge (EoC) state, which is, of course, rate dependent. Therefore, the disparity in the capacity is predominantly governed by the charge regime.

Scenario (c), as displayed in Fig. 2(c), is a conciliation of the previous two, where the kinetics played a more complex role leading to the composition (primarily in cathode) of the system fluctuating between the fully lithiated and unlithiated states at different rates. An appropriate model to describe this behavior is a dynamic "shrinking core model" typically used to explain the progression of solid state reaction in a solid particle in terms of chronicle consequence of product evolution.

In the last two scenarios, it should be noted that the difference between t-SoC and e-SoC becomes apparent. This is what has been a troubling issue in the determination of SoC.

To fully exploit this issue, in lieu of which scenario is most likely the one that describes the correct pathway for the charge discharge behavior, the following experiments and analyses were conducted:

The experiment involves a series of charge and discharge cycles at different rates to deduce the corresponding t-SoC. Fig. 3 presents a sequence of cycling events in which the LCO cell was first charged at *C*/25 (curve ①), then cycled at *C*/5 (curves ❷ –❻ , in which odd numbers are charge regimes and even numbers are discharge regimes, all at *C*/5 rate), and finally recharged again at *C*/25 (curve ⑦). It should be noted that the charge at *C*/25 in curve ⑦ is a replication of the same regime as in curve ① . The subsequent *C*/5 cycles from ❷ to ❻ are symmetrical and reversible; thus, disregarding if the series is from ① to ⑦ or inversely from ⑦ to ① , the results should be identical.

The figure shows that either charge or discharge curves that correspond to the same rate coincide with one another. It is reproducible and consistent with coulomb counting without any noticeable charge loss. As such, tallying the amount of charge in and out of the cell at different rates can account for the discrepancy between C_{25} and C_5 mainly in the EoC state. In other words, it becomes apparent that all discharge curves reach the

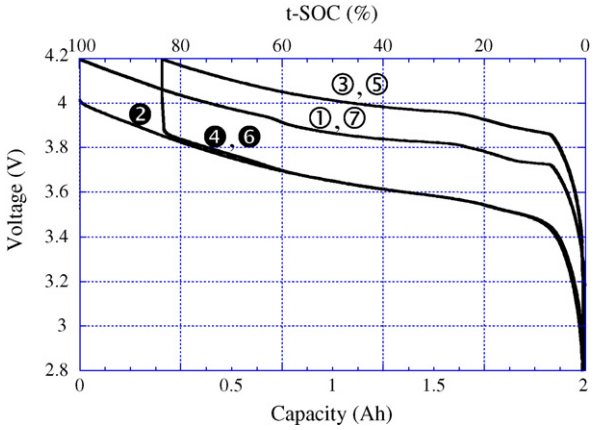

Fig. 3. A series of charge discharge curves measured on the LCO cell with the following chronicle order: curve ① charge at *C*/25, ❷ discharge at *C*/5, ③ charge at *C*/5, ❹ discharge at *C*/5, ⑤ charge at *C*/5, ❻ discharge at *C*/5, and ⑦ charge at *C*/25. The coulomb counting of capacity is clearly demonstrated. The related SoC change can be inferred from the SoC scale on the top.

same EoD state, independent of either charge or discharge rate. It is also clear that the *C*/25 and *C*/5 cycles can be executed reversibly (per curves ① –❷ –⑦ and ③ –❻ , respectively), but C_5 only accounts for 84% of C_{25}, almost exclusively due to the difference in the EoC state. As the result of this analysis, we can now assign the t-SoC scale to the charge and discharge curves, as shown in the upper scale of Fig. 3.

From Fig. 3 and the above analysis, it appears plausible that at the end of *C*/5 charging (③ or ⑤) additional capacity may be available if the cell were allowed to be charged at a lower rate (as shown by ⑦). We thus performed an ICA using the data displayed in Figs. 1 and 3. The results are shown in Fig. 4, in which the *C*/25 cycle (from Fig. 1) is depicted in dashed lines, while those from the *C*/5 experiments in Fig. 3 are in solids. Three dominant incremental capacity (IC) peaks are observed. The origin of these three peaks can be analyzed as follows: there is a predominant phase transformation on CAM, which gives the nominal 3.8 V plateau. The graphite anode has three staging processes evolved through the entire capacity range. Therefore, the three IC peaks primarily come from the anode staging. The separations among the peaks also correspond to the potential differences exhibited in the anode staging. The position, shape, height and width of each peak depend on the nature of the staging reaction and the associated kinetics; therefore, they are most likely rate-dependent. Based on the IC curve of *C*/25 (derived from Fig. 1), we can conclude that the pair of IC peaks intersect at 3.81 V is related to the primary phase transformation in the LCO chemistry. The second pair of prominent peaks at 3.71 V is related to the same phase transformation, but was split from the primary pair due to the staging in the graphite anode. The solid solution region is the broad band above 3.9 V with an onset between the charge and discharge branches close to 3.92 V. This solid solution regime does not terminate even at 4.2 V. Knowing the features on the IC curve, we can infer the rate dependent behavior in the IC responses upon cycling as depicted by those in Fig. 3.

With what has been postulated in Fig. 3, we further infer that the higher polarization with *C*/5 (than *C*/25) leaves a portion of the solid solution formation beyond the EoCV (curves ③ and ⑤) and the corresponding capacity becomes unavailable at this rate. Thus, the incomplete recharge leads to less capacity at this

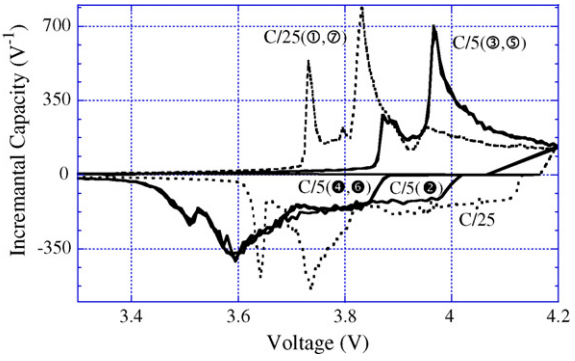

Fig. 4. An incremental capacity analysis (ICA) of the data shown in Figs. 1 and 3. The IC curves of *C*/25 charge and discharge regimes are shown in dashed lines, and the *C*/5 curves (taken from curve ❷ –❻ in Fig. 3) are shown in solid lines.

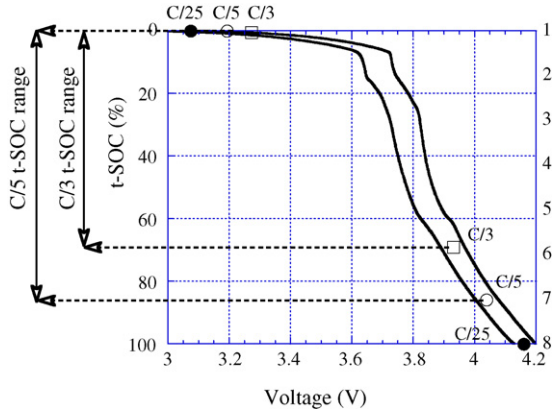

Fig. 5. Close-to-equilibrium OCV (*cte*-OCV) measurements of the LCO cell at the end-of-charge and end-of-discharge conditions at *C*/25, *C*/5 and *C*/3 charge and discharge regimes, respectively. Excursion of SoC in the cell is clearly illustrated.

rate. The inaccessible capacity may become available if the cell were charged at a rate slow enough to allow full reaction of the unreacted portion of the solid solution. This is exactly what transpired in curve ❷ , which depicts a *C*/5 discharge after a *C*/25 charge. Curve ❷ follows other *C*/5 discharges (i.e. ❹ and ❻) except the portion above 3.84 V where the additional solid solution capacity is present.

Finally, all the above-mentioned hypotheses and deductions are put to attestation by the *cte*-OCV measurements, which allow the t-SoC to be determined and validated. This approach allows the cell to reach equilibrium when resting, so equilibrium t-SoC can be determined. Fig. 5 presents the *C*/25 charge and discharge curve as well as the *cte*-OCV of *C*/25 (●), *C*/5 (◯), and *C*/3 (□) at the EoD and EoC, respectively. The *cte*-OCV for each EoD condition clearly confirms our postulation that the discharge regime at different rates reaches almost the same EoD composition, or the variants are truly negligible. On the contrary, the *cte*-OCV for each EoC condition at different rates displays the vast disparities in the t-SoC's, and thus the capacity. The origin of the disparity from the charge regime is clearly identified. The projected C_5 and C_3 are about 84% and 69% of C_{25}. These results are consistent with those measured experimentally from the discharge regime.

4. Conclusion

A clear explanation of the relationship between cell rate-dependent capacity and SoC is achieved in this work. The translation of e-SoC to t-SoC has been proven to be important in order to reflect the real changes in the active material in a battery with rate and upon cycling. This realization is also essential to establish a good model for battery performance and life prediction.

Such understanding of the relationship between rate-dependent capacity and SoC can be achieved using several experimental and analytic techniques. In this paper we presented three techniques that can be utilized to reveal such

a relationship. The first one is a well crafted and executed charge discharge cycles with various rates to tally the coulomb counting with respect to rate change. This approach can reveal the capacity differences in relevance to the rate and the end-of-charge (EoC) and end-of-discharge (EoD) states. Another useful and definitive technique is the close-to-equilibrium OCV (*cte*-OCV) measurements and analysis, which directly determine the SoC in equilibrium in the cell with respect to any charge and discharge regimes. This measurement will provide a reliable reference point for any subsequent analysis of the cell behavior with SoC. This *cte*-OCV measurement in conjunction with the coulomb counting approach in cycling can yield full understanding of the cell polarization performance with accurate SoC information. The last approach demonstrated in this work is the incremental capacity analysis. The evolution of the incremental capacity peaks under various cycling rates can provide an overall view of how the kinetics affects the capacity inventory and help to infer the subsequent SoC estimates.

Acknowledgements

This work is performed under a contract (HEVDP contract #46049, Supplement 5) with the Hawaii Center for Advanced Transportation Technologies (HCATT) under the support (Federal Other Transaction Agreement No. DTRS56-99-T-0017) from the U.S. Air Force Advanced Power Technology Office (APTO) at the Robins Air Force Base in Georgia.

References

[1] M. Dubarry, V. Svoboda, R. Hwu, B.Y. Liaw, Electrochem. Solid State Lett. 9 (2006) A454.
[2] J. Barker, Electrochim. Acta 40 (1995) 1603.
[3] J. Barker, M.Y. Saidi, R. Koksbang, Electrochim. Acta 41 (1996) 2639.
[4] J. Barker, R. Koksbang, M.Y. Saidi, Solid State Ionics 89 (1996) 25.
[5] Electric Vehicle Battery Test Procedures Manual, U.S. Advanced Battery Consortium (USABC) and U.S. Department of Energy (US DOE), Idaho National Laboratory (INEEL), Revision 2, January 1996.
[6] T. Hansen, C.-J. Wang, J. Power Sources 141 (2005) 351.
[7] S. Piller, M. Perrin, J. Power Sources 96 (2001) 113.
[8] G.L. Plett, Proceedings of the EVS 20 Symposium, Long Beach, CA, November 15–19, 2003.
[9] G.L. Plett, J. Power Sources 134 (2004) 277.
[10] S. Pang, J. Farrell, J. Du, M. Barth, Proceedings of the American Control Conference, Arlington, 2001.
[11] C.H. Cai, D. Du, Z.Y. Liu, Poster Presentation at the IEEE International Conference on Fuzzy Systems, St. Louis, 2003.
[12] W. Weppner, R.A. Huggins, J. Electrochem. Soc. 124 (1977) 1569.
[13] C.J. Wen, C. Ho, B.A. Boukamp, I.D. Raistrick, W. Weppner, R.A. Huggins, Int. Met. Rev. 5 (1981) 253.
[14] B.Y. Liaw, I.D. Raistrick, R.A. Huggins, Solid State Ionics 45 (1991) 323.
[15] B.Y. Liaw, in: J. Nowotny, C.C. Sorrell (Eds.), Electrical Properties of Oxide Materials, Key Engineering Materials Series, vols. 125–126, Trans. Tech. Publications, Switzerland, 1996, p. 133.
[16] X.G. Yang, B.Y. Liaw, J. Power Sources 102 (2001) 186.
[17] B.Y. Liaw, G. Nagasubramanian, R.G. Jungst, D.H. Doughty, Solid State Ionics 175 (2004) 835.
[18] B.Y. Liaw, R.G. Jungst, G. Nagasubramanian, H.L. Case, D.H. Doughty, J. Power Sources 140 (2005) 157.
[19] M. Dubarry, B.Y. Liaw, J. Power Sources 174 (2007) 856.